

Indian Institute of Space Science and Technology  
Department of Aerospace Engineering

# Natural and Forced Characteristics of Circular and Elliptic Jet Diffusion Flames

Priy Devvrat Singh

May 3, 2018

# Content



## Introduction

### Objective

## Experimental Methods

### Setup

Flow visualization technique

Image processing

## Signal and Data Analysis Techniques

Non-linear Time Series Analysis

Dynamic Mode Decomposition

## Natural Characteristics

General Characteristics

Effect of AR on Natural Frequency

## Forced Characteristics

Forcing near the natural frequency:  $F_n$

Forcing near the first subharmonic:  $F_n/2$

## Summary and Conclusion

# Objective



2

- ▶ To understand natural unsteady characteristics of jet diffusion flames and the effect of AR on it.
- ▶ To understand response of diffusion flame to acoustic forcing and the variation of response with AR of nozzle.

# Setup

## Experimental Methods

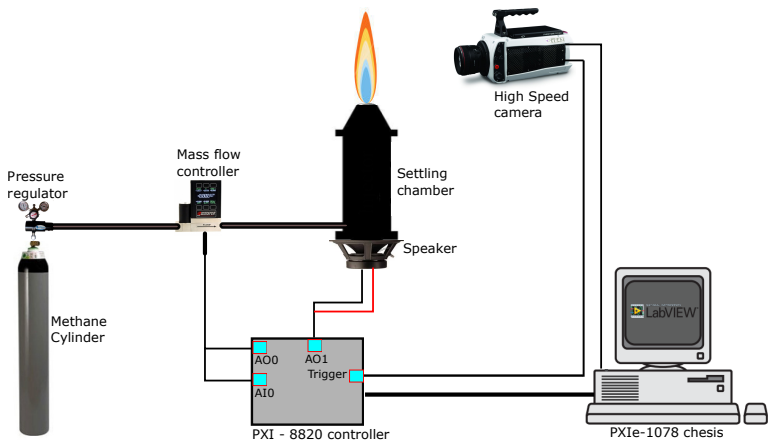


**Figure:** Schematic of the experimental setup.

# Flow visualization technique

## Experimental Methods

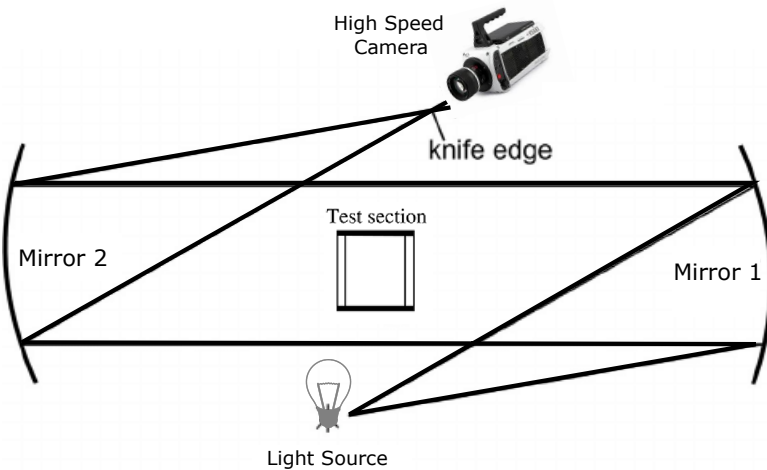


**Figure:** Schematic of Z type schlieren setup.

# Image processing

## Experimental Methods



5

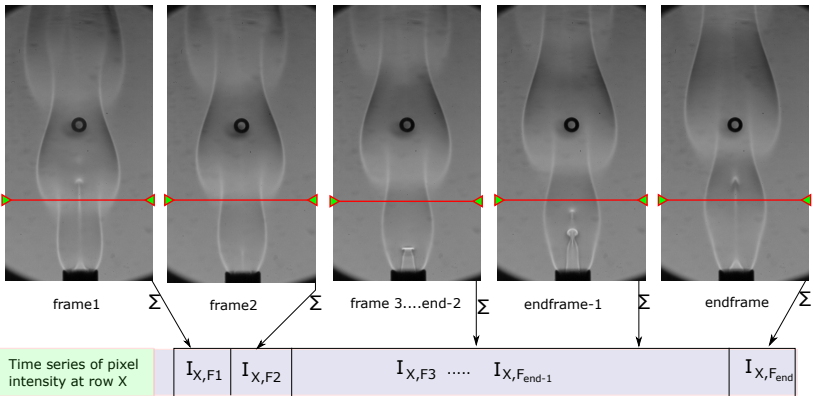


**Figure:** Representation of procedure to obtain time series data of flame intensity at  $x/D = 10$  location.

# Non-linear Time Series Analysis

## Signal and Data Analysis Techniques

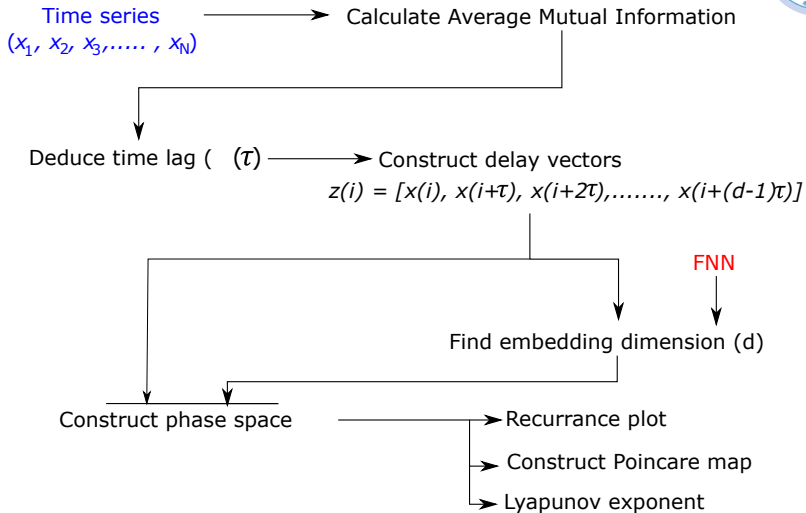
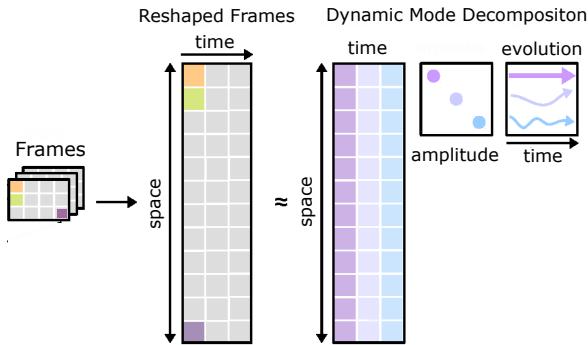


Figure: Flowchart of non-linear time series analysis procedure.

# Dynamic Mode Decomposition

Signal and Data Analysis Techniques



- ▶ Dynamic Mode Decomposition (DMD) provides a means to decompose time-resolved data into modes, with each mode having a single characteristic frequency of oscillation and growth/decay rate.
- ▶ DMD is helpful for both description and prediction.

# Natural Unsteady Characteristics

General flow field behavior

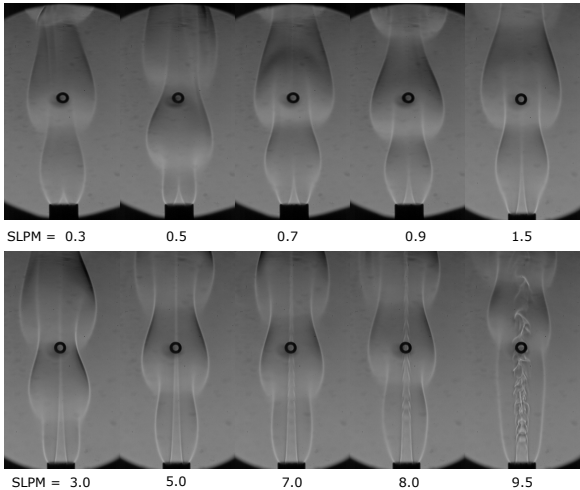


**Figure:** Variation of schlieren flow field with flow rate for  $AR = 3$  elliptic flame.

# Natural Unsteady Characteristics

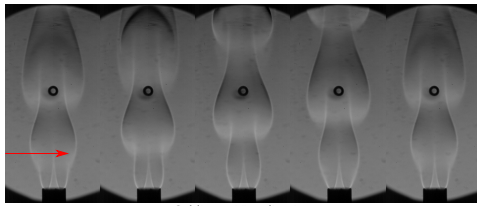
General flow field behavior



9



Direct Chemiluminescence Visualization



Schlieren Visualization

**Figure:** Image sequence of natural oscillations as seen from major axis side for flame from AR = 3 elliptic nozzle.

# Natural Unsteady Characteristics

General flow field behavior



**Results discussed for AR = 2, Re = 239 case.  
Spatial Variation of frequency**

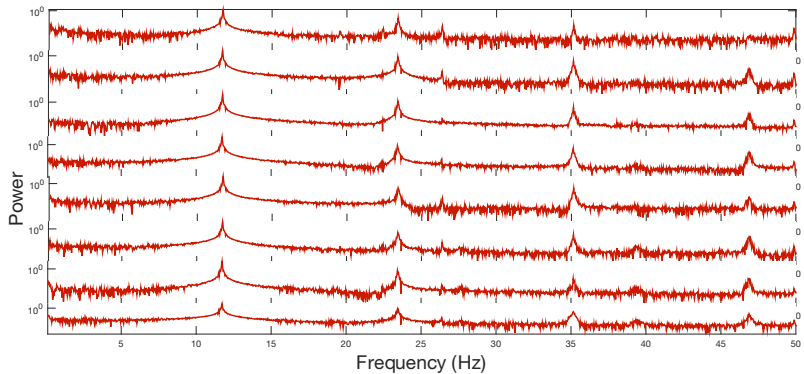


**Figure:** Power spectrum plot of signal at  $x/D = (5,10,15,20,25,30,35,40)$  locations.

# Natural Unsteady Characteristics

General flow field behavior



## Temporal variation of frequency

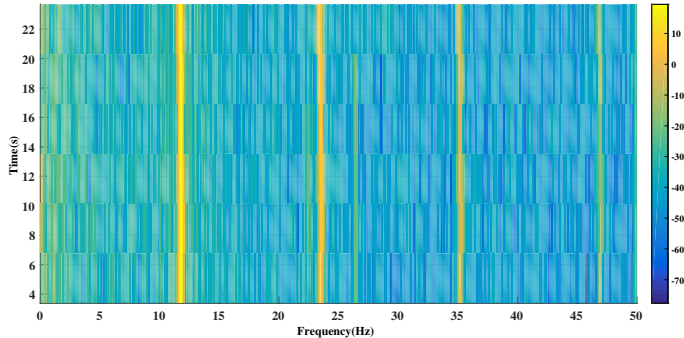


**Figure:** Spectrogram plot for time series signal at  $x/D = 10$ ,  $AR = 2$ ,  $Re = 239$ , natural oscillations case

# Results from Non-linear time series analysis



12

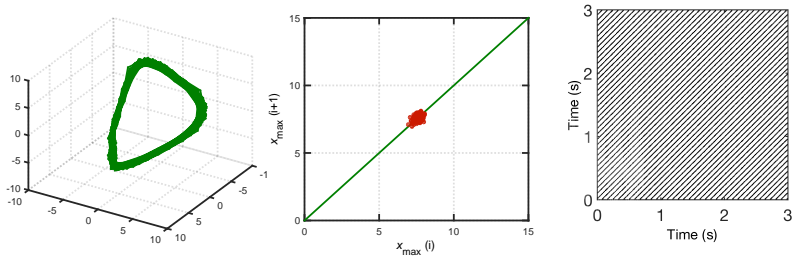


**Figure:** (a) 3D phase portrait (b) Poincaré map and (c) Recurrence plot for time series signal for flame with AR = 2 and Re = 239.

# Results from DMD



13

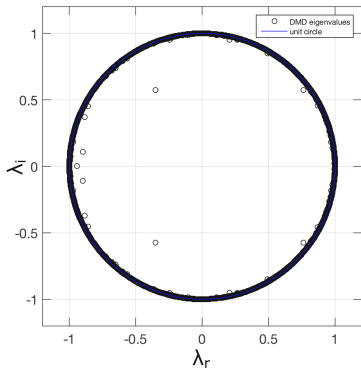
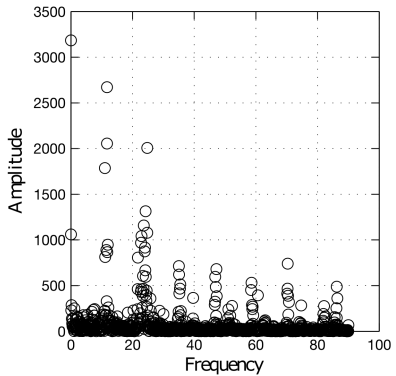


**Figure:** (a) DMD spectrum and (b) Eigenvalue visualization for flame with AR = 2 nozzle, Re = 239, major side flow visualization.

# Results from DMD



14

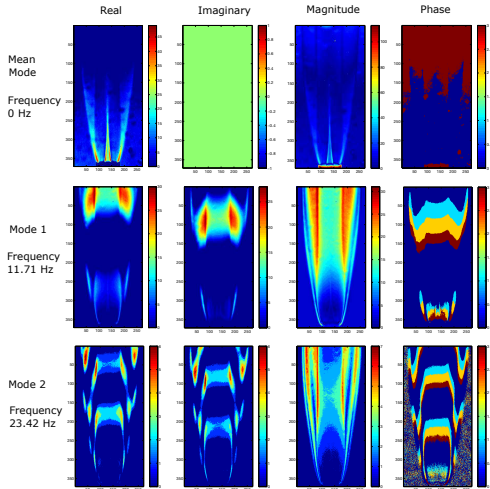


**Figure:** Spatial characteristics of mean and first 2 DMD modes for AR=2, Re = 239, major axis side case.

# Effect of AR on natural unsteady characteristics



- ▶ Objective is to find a correlation between  $St$  and  $Fr$
- ▶ How does this correlation vary with AR?
- ▶ To find a universal scaling, if exist.

Defined as

$$St = fD/V, Fr = V^2/gD \quad (1)$$

Let

$$St = K_1(1/Fr)^m$$

and

$$St = K_2(Re)^n$$

$$f \propto \frac{g^m D^{m-1}}{V^{2m-1}} \quad (2)$$

# Correlations with $D = 2\sqrt{ab}$

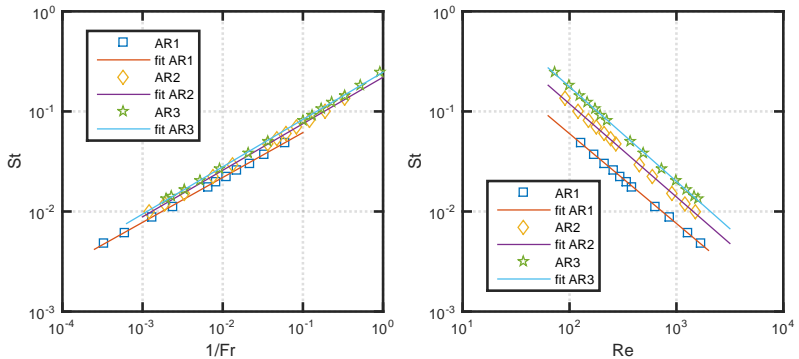


**Figure:** (a) Strouhal number vs Froude number, (b) Strouhal number vs Reynolds number for natural oscillations in case of AR = 1, 2, 3 nozzles. The characteristic length  $D$  is  $2\sqrt{ab}$ .

# Effect of AR



Table: Power law fit for  $D = 2\sqrt{ab}$

nozzle	St vs Fr		St vs Re	
	exponent (m)	Intercept ( $K_1$ )	exponent (n)	Intercept ( $K_2$ )
Circular	0.4485	0.1726	-0.8970	3.7273
Elliptic AR = 2	0.4650	0.2197	-0.9301	8.6211
Elliptic AR = 3	0.4726	0.2465	-0.9451	13.6765

Table: Power law fit for  $D = 2b$

Nozzle	St vs Fr		St vs Re	
	exponent (m)	Intercept ( $K_1$ )	exponent (n)	Intercept ( $K_2$ )
All AR	0.4694	0.1916	-0.9387	4.7748

# Correlations with $D = 2b$

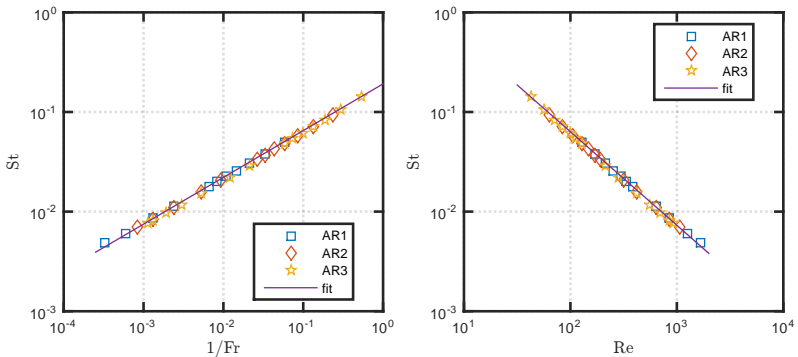


**Figure:** (a) Strouhal number vs Froude number, (b) Strouhal number vs Reynolds number for natural oscillations in case of AR = 1, 2, 3 nozzles. The characteristic length  $D$  is  $2b$ .

# Forced Characteristics



**Table:** All flames used for acoustic excitation

Flame	Nozzle	Flow rate	Velocity	Re	Natural Frequency ( $F_n$ )
		SLPM	m/sec		Hz
1	Circular	0.7	1.6505	295.74	12.42
2	Elliptic AR = 2	0.8	0.9431	239	11.73
3	Elliptic AR = 3	0.9	0.7074	219.52	11.26

# Forcing near the natural frequency

Forced characteristics



20

**Circular flame forced at  $F_f/F_n=0.95$ .**

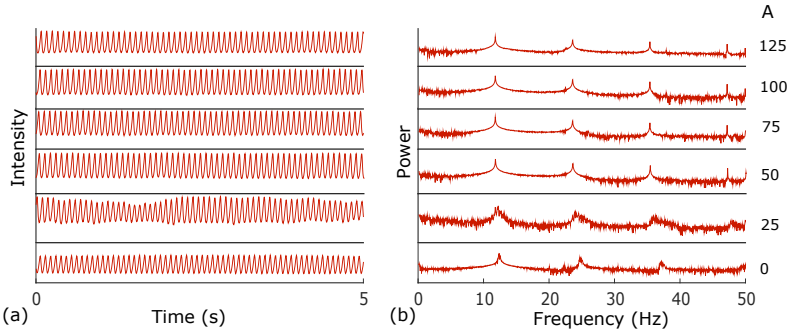


**Figure:** (a) Time series (b) power spectrum of intensity for circular flame forced at  $F_f = 11.8$  Hz, slightly below the natural frequency,  $F_n = 12.42$  Hz;  $F_f/F_n=0.95$ .

# Forcing near the natural frequency

Circular flame forced at  $F_f/F_n=0.95$ .



21

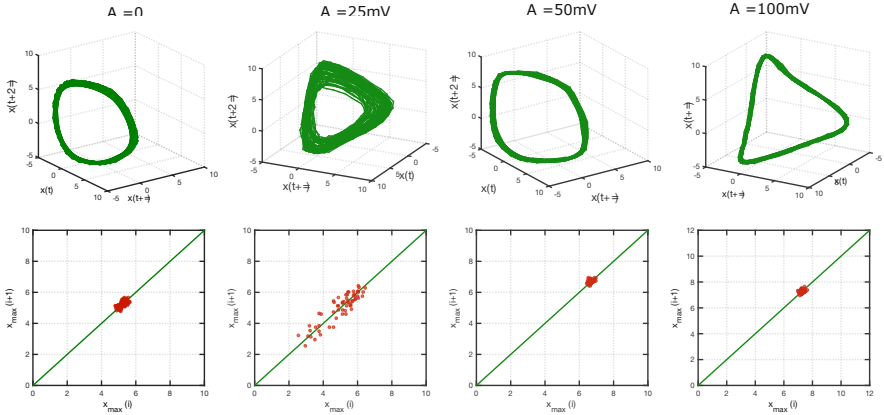


**Figure:** (a) 3D phase portrait (b) Poincaré map for circular flame forced at  $F_f = 11.8$  Hz, slightly below the natural frequency,  $F_n = 12.42$  Hz:  $F_f/F_n=0.95$ .  $A_{loc} = 50$  mV

# Forcing near the natural frequency

Forced characteristics



22

**Circular flame forced at  $F_f/F_n=1.0869$**

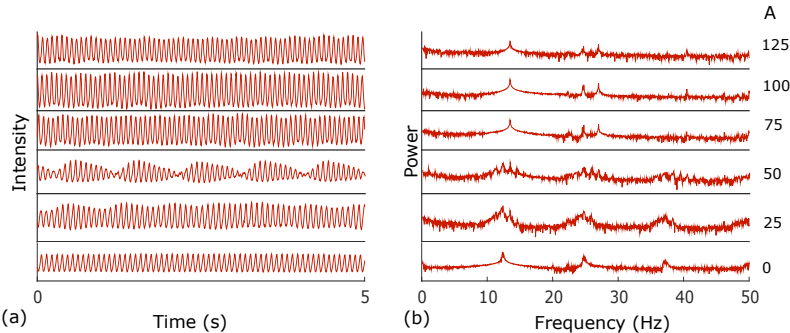


**Figure:** (a) Time series (b) power spectrum of intensity for circular flame forced at  $F_f = 13.5$  Hz, slightly above the natural frequency,  $F_n = 12.42$  Hz:  $F_f/F_n = 1.0869$ .  $A_{loc} = 75$  mV

# Forcing near the natural frequency

Forced characteristics



23

**Circular flame forced at  $F_f/F_n = 0.8454$**

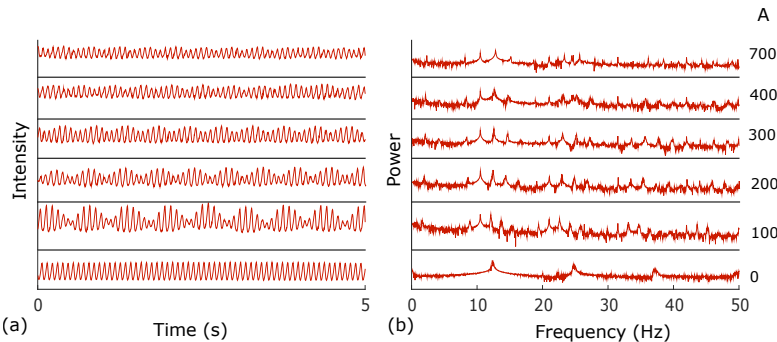


**Figure:** (a) Time series (b) power spectrum of intensity for circular flame forced at  $F_f = 10.5$  Hz:  $F_f/F_n = 0.523$ . The amplitude shown is in mV.

# Forcing near the natural frequency

Circular flame forced at  $F_f/F_n = 0.8454$



24

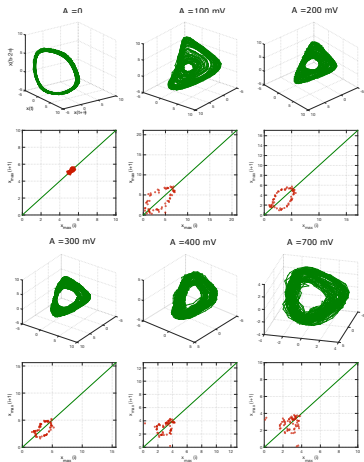


**Figure:** (a) 3D phase portrait (b) Poincaré map for circular flame forced at  $F_f = 10.5$  Hz:  $F_f/F_n = 0.8454$ .

# Forcing near the first subharmonic: $F_n/2$

Forced characteristics



25

**Circular flame forced at  $F_f/F_n=0.523$**

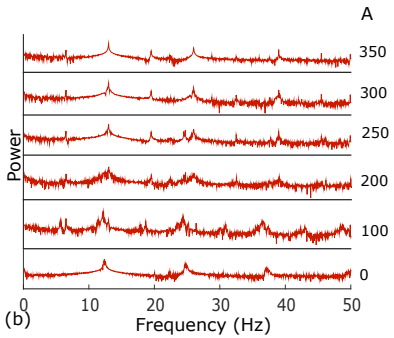
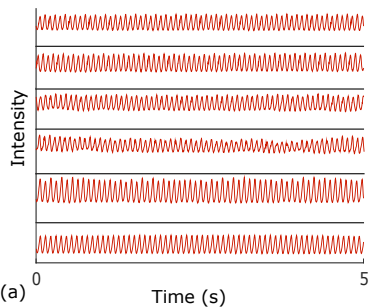


**Figure:** (a) Time series (b) power spectrum of intensity for circular flame forced at  $F_f = 6.5$  Hz, slightly above the first subharmonic of natural frequency,  $F_n = 12.42$  Hz:  $F_f/F_n = 0.523$ .  $A_{loc} = 300$  mV

# Forcing near the first subharmonic: $F_n/2$

Circular flame forced at  $F_f/F_n=0.523$ .

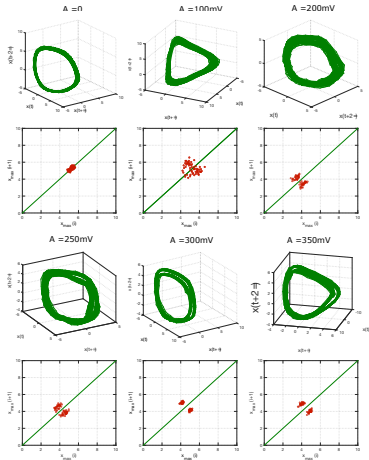


**Figure:** (a) 3D phase portrait (b) Poincaré map for circular flame forced at  $F_f = 6.5$  Hz:  $F_f/F_n=0.523$ .  $A_{loc}= 300$  mV

# Forcing near the first subharmonic: $F_n/2$

AR = 3 elliptic flame forced at  $F_f/F_n=0.5417$

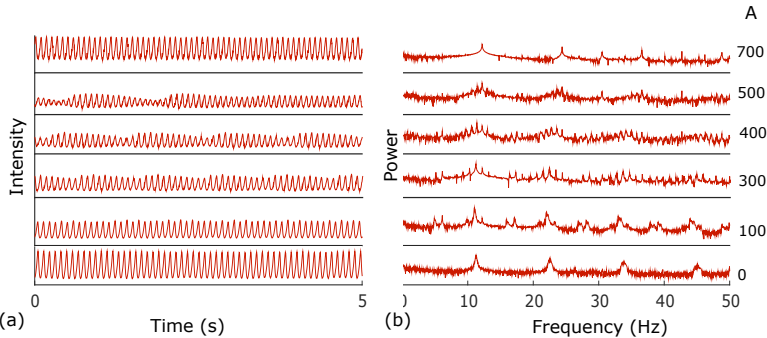


**Figure:** (a) Time series (b) power spectrum of intensity for flame 3 (elliptic AR = 3 nozzle) when forced at  $F_f = 6.1$  Hz:  $F_f/F_n= 0.5417$ . The amplitude shown is in mV.  $A_{loc} = 700$  mV

# Forcing near the first subharmonic: $F_n/2$

AR = 3 elliptic flame forced at  $F_f/F_n = 0.5417$ .

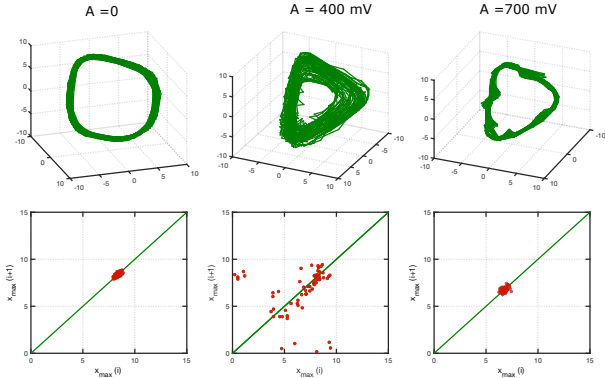


**Figure:** (a) 3D phase portrait (b) Poincaré map for flame 3 (AR = 3, Re = 219.52) forced at  $F_f = 6.1$  Hz:  $F_f/F_n = 0.5417$ .

# Results from DMD

Circular flame forced at  $F_f = 6.5$  Hz with  $A = 0.1$  V



29

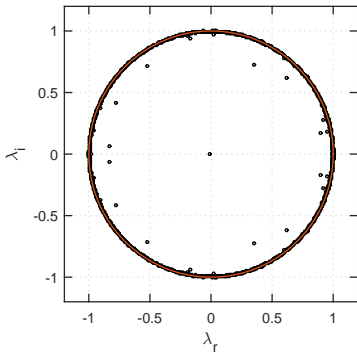
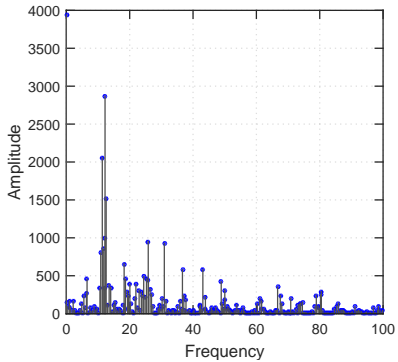


**Figure:** (a) DMD spectrum, (b) eigenvalue visualization for flame 1 when forced at  $F_f = 6.5$  Hz and  $A = 100$  mV.

# Results from DMD

Circular flame forced at  $F_f = 6.5$  Hz with  $A = 0.1$  V

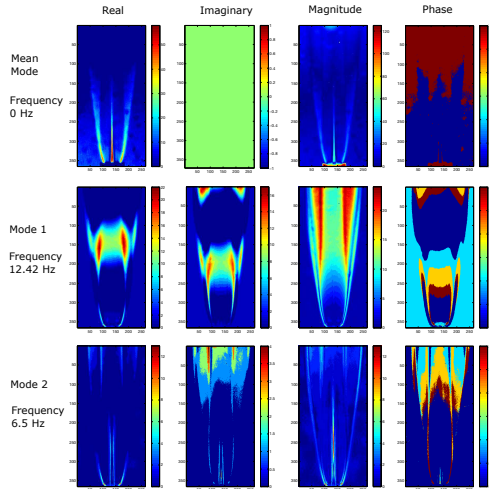


**Figure:** Spatial characteristics of mean, natural and forcing modes for AR=1, Re = 295.74, when forced at 6.5 hz with  $A = 100$  mV



- ▶ High speed schlieren flow visualization was used to capture flame response in natural as well as acoustically excited cases for AR = 1, 2, 3 elliptic jet diffusion flames.
- ▶ Non-linear time series analysis was used to understand topology of dynamic system.
- ▶ DMD analysis was done to understand spatial structures of natural, forced modes and modes generated as a result of non-linear interaction between  $F_f$  and  $F_n$ .

# Conclusion



- ▶ Frequency dependence on velocity was found to be maximum for circular and dependence reduced as AR increases.
- ▶ A single correlation and scaling between  $St$  and  $Fr$  was found which was able to capture unsteady characteristics of all elliptic and circular flames.
- ▶ Lock-in route through phase locked was observed for circular and elliptic nozzle when forced near fundamental frequency.
- ▶ A period doubling route to lock-in was observed for circular nozzle when excited near the first sub-harmonic of fundamental frequency.
- ▶ when elliptic flames were excited near the first sub-harmonic, it showed a phase locked route to lock in and the forcing frequency disappears from the system.

A large, stylized graphic element in the upper right corner of the slide. It consists of several thick, curved lines in shades of blue, teal, and orange. The lines curve from the top left towards the bottom right, creating a sense of motion. Some smaller, thinner lines extend from the main cluster on the right side.

**Thank you**